ACS Sustainable Chemistry & Engineering

Research Article

pubs.acs.org/journal/ascecg

Improved Photoelectrical Performance of Single-Crystal TiO_2 Nanorod Arrays by Surface Sensitization with Copper Quantum Dots

Qiong Sun,[†] Yang Li,[†] Xianmiao Sun,[†] and Lifeng Dong*[,†,‡]

[†]College of Materials Science and Engineering, Qingdao University of Science and Technology, Qingdao, 266042 P.R. China

[‡]Department of Physics, Astronomy, and Materials Science, Missouri State University, Springfield, Missouri, 65897, United States

ABSTRACT: Through the redox reaction between Cu-$(NH_3)_4^{2+}$ and H_2O_2, copper quantum dots (QDs) were deposited onto the surface of single-crystal rutile TiO_2 nanorod arrays that were grown directly on transparent, conductive fluorine-doped tin oxide substrates by a facile hydrothermal process. Compared with pristine TiO_2 nanorods, the top facets of TiO_2 nanorods decorated with Cu QDs became flattened and adherent to each other, and the lateral facets were rough and covered with vast amounts of extremely small particles. The QDs were tightly attached on the surface of the nanorods, and the nanoparticle size measured from high resolution transmission electron microscopy images was around 6 nm, which is comparable with the Bohr exciton radius. X-ray photoelectron spectroscopy measurements showed that the QDs existed in the form of Cu(II)O and $Cu(I)_2O$ after the deposition process, and the Cu(0) QDs were unstable on the TiO_2 surface. Furthermore, under the irradiation of a solar simulator, the photocurrent response of the QD sensitized TiO_2 nanorods was improved dramatically with a small amount of QDs, and the optimal photocurrent density (98 $\mu A/cm^2$) was much greater than that of the undecorated sample (16 $\mu A/cm^2$). Likewise, external quantum efficiency (EQE) characterization demonstrated the superiority of the surface modification with Cu QDs, by which the highest EQE value of the photoanode was enhanced nearly ten times. In addition, a red shift of the peak in EQE measurement was found from the Cu QD sensitized samples, suggesting a quantum size effect caused by small QD particles.

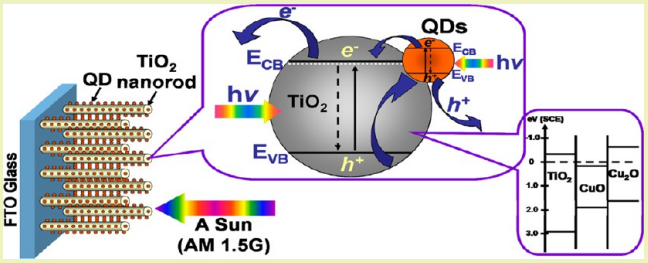

KEYWORDS: *Copper quantum dots, TiO_2 nanorod arrays, Surface sensitization, Photoelectrical conversion*

INTRODUCTION

In order to extend the applications of solar cells in more regions, much effort has been devoted to developing a new generation of low cost sensitized solar cells, including dye-sensitized solar cells (DSSCs)[1−4] and quantum-dot-sensitized solar cells (QDSCs).[5−7] For the past two decades, cost-performance compatible DSSCs have attracted a great deal of attention as the essential components in the third generation of solar cells. DSSCs are based on the photosensitization of nanocrystalline TiO_2 semiconductor electrodes by absorbed dyes.[8] One common factor determining the efficiency of a DSSC is the light harvesting ability of the dye attached to the TiO_2 surface.[9] The most used photosensitive dyes, pyridine or porphyrin-based macrocyclic complexes with rare metals (e. g., Ru) in their centers, demonstrate a substantial photoelectrical conversion efficiency of up to 13%.[10] However, these sensitizers are difficult to synthesize and purify, and the use of rare metals makes them relatively expensive compared with conventional power sources.[11]

As an alternative sensitizer, semiconductor quantum dots (QDs) attract great interest. The QDs have size-dependent separation between the valence and conduction bands and discrete exciton-like states.[12] In contrast with organic and organometallic sensitizers, a lot of QDs exhibit unique size-dependent electronic and optical features, such as a tunable band gap, high extinction coefficients, multiple exciton generation (MEG), and an expanding optical absorption range by reducing the particle size smaller than Bohr radius.[13−15] Many QDs have been thoroughly investigated with regard to their photoelectrical activity on TiO_2 surfaces, including CdS,[16] CdSe,[17] PbS,[18] PbSe,[19] InAs,[20] and InP.[21] Recently, TiO_2 QDSCs assembled with colloidal PbS quantum dots demonstrated a photoelectrical efficiency of ∼6% under the irradiation of an AM 1.5G solar simulator, supposedly the highest value generated among existing QDSCs.[22]

However, the QDs extensively studied above usually contain some toxic element or rare element, such as Cd, Pb, and In, which can cause potential environmental and health problems. As a result, it is necessary to discover eco-friendly QD materials. For instance, because of its various advantages, such as low cost, low toxicity, abundance, and ability to be coupled with a wide band gap semiconductor, cupric compounds have been doped into TiO_2 to enhance its photocatalytic or photoelectrical activity.[23,24] Recently, cupric quantum dots have attracted

Special Issue: Sustainable Nanotechnology

Received: April 4, 2013
Revised: May 23, 2013
Published: May 27, 2013

increasing attention for their applications in solar cells, including Cu_2O,[25] CuS,[26] and $CuInS_2$.[27] In our recent research,[28] we synthesized a series of cupric quantum dots (e.g., Cu, CuO, CuS, Cu_2O, and Cu_2S) on the surface of TiO_2 nanoparticles and studied the morphologies and photovoltaic properties of the QD-modified TiO_2 nanoparticles. Among these cupric QDs above, the elementary Cu QDs yielded the best photoelectric characteristics in the surface modified TiO_2 nanoparticles, a result that could, hypothetically, be due to both the formation of a Cu(I)/Cu(II)−O−TiO_2 network on the TiO_2 surface and the matched energy levels between Cu QDs and TiO_2. As an emerging photoelectric material, the Cu QD-sensitized TiO_2 will undoubtedly receive more attention in the near future.

Since Aydil presented a facile hydrothermal reaction for the direct synthesis of TiO_2 nanorod arrays, the grown in situ TiO_2 nanorods have been widely used in the preparation of photoanodes due to their excellent photovoltaic properties.[29−31] In our recent work, we systematically investigated effects of a number of experimental parameters on the morphologies and photoelectrical conversion abilities of pristine TiO_2 nanorods, such as growth time, reaction temperature, pH value, titanium precursor type and concentration, and sintering treatment.[32−34] Among them, the role of temperature during the nanorod synthesis and sintering process was emphasized.

Until now, no report about the surface sensitization of TiO_2 nanorod arrays with copper QDs exists to our knowledge. In this study, oriented TiO_2 nanorod arrays were formed first on transparent conductive fluorine-doped tin oxide (FTO) substrates, and elementary Cu QDs were subsequently produced by a solution chemical redox method. Finally, the oxidized Cu QDs with extremely small size were dispersed evenly on the surface of TiO_2 nanorods. The morphology and structures of QDs and TiO_2 nanorods were characterized using X-ray diffraction (XRD), field emission scanning electron microscopy (FESEM), high resolution transmission electron microscopy (HRTEM), energy dispersive X-ray spectroscopy (EDS), and X-ray photoelectron spectroscopy (XPS). Furthermore, the photoelectrical conversion ability of QD-TiO_2 nanorods were discussed, and it was found that a small amount of QDs can significantly improve the performance due to the coexistence of Cu(II)O and $Cu(I)_2O$ QDs.

EXPERIMENTAL SECTION

Deionized and double distilled water was used throughout this study, and the reagents were used as received without further purification.

Hydrothermal Synthesis of TiO_2 Nanorod Arrays. Oriented TiO_2 nanorod arrays were synthesized on FTO substrates by a hydrothermal process.[32−34] Briefly, 30 mL of deionized water was mixed with 30 mL of concentrated hydrochloric acid (36.5%) in a Teflon-lined stainless steel autoclave (100 mL). The mixture was stirred for 5 min under ambient conditions prior to the addition of 1.2 mL titanium isopropoxide [Ti(*i*Pro)$_4$] as titanium precursor, and then, the mixture was stirred for another 5 min. A piece of FTO substrate was ultrasonically cleaned in the sequence of deionized water, acetone, and ethanol, each for 10 min, and was placed at an angle against the wall of the Teflon liner with the conducting side facing down. TiO_2 nanorod arrays were synthesized through the hydrothermal process at 155 °C for 4 h. After being cooled to room temperature under dripping water for 30 min, FTO substrates were removed from the autoclave and washed with deionized water, then dried in ambient air and stored in the dark.

Immobilization of Copper Quantum Dots (Cu QDs) onto TiO_2 Nanorods. Copper QDs were obtained by using copper acetate ($Cu(AC)_2$), hydrogen peroxide (H_2O_2), and ammonia ($NH_3{\cdot}H_2O$) as reaction precursors through a redox reaction as below:[35]

$$Cu(AC)_2 + 6NH_3{\cdot}H_2O \rightarrow Cu(NH_3)_4^{2+} + 2NH_4AC + 2OH^- + 4H_2O \quad (1)$$

$$Cu(NH_3)_4^{2+} + H_2O_2 + 2OH^- \rightarrow Cu + O_2 + 4NH_3 + 2H_2O \quad (2)$$

For the surface sensitization process, different concentrations of $Cu(NH_3)_4^{2+}$ (resulting from $Cu(AC)_2$ and $NH_3{\cdot}H_2O$) and H_2O_2 aqueous solutions were prepared in two beakers, respectively. A piece of FTO substrate, with TiO_2 nanorods attached on the conducting side, was dipped into one beaker containing the dark blue $Cu(NH_3)_4^{2+}$ solution, at an angle against the wall with the TiO_2 side facing up. After the adsorption of $Cu(NH_3)_4^{2+}$ on the TiO_2 surface for 2 min, the sample was extracted and washed with deionized water, then dipped into H_2O_2 in the other beaker for 2 min to produce elemental copper QDs on the TiO_2 surfaces. After 10 cycles of the redox reaction, the color of the product changed from white to yellow−green (Figure 1). The modified TiO_2 nanorod arrays on FTO were then dried in ambient air and stored in the dark.

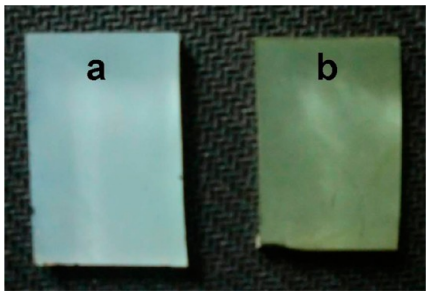

Figure 1. Photograph of (a) pristine TiO_2 film and (b) Cu QD sensitized TiO_2 film on FTO substrate (0.05 M Cu^{2+} in reactant).

Characterization. Fine lattice structural information of TiO_2 was obtained by HRTEM (FEI Tecnai G2 F20) and selected area electron diffraction (SAED) with an accelerating voltage of 200 kV. For the HRTEM characterizations, the sample was first added into ethanol solution and, then, dispersed in an ultrasonic cleaner for 15 min. The suspension was dropped onto a copper TEM grid and dried in ambient air at room temperature.

Crystal compositions of Cu-TiO_2 were detected on a D/max-rA diffractometer (Rigaku, D/MAX-2500/*Pc*), using Cu Kα as the X-ray source (40 kV, 100 mA). FESEM (Jeol JSM-6700F) was chosen to observe the surface morphology of Cu-sensitized TiO_2 nanorod arrays on the FTO substrata, and the elemental distribution and concentration were analyzed by EDS (Oxford Inca) attached to the FESEM. XPS (Kratos Analytical Ltd., Axis Ultra) measurements were conducted to investigate chemical status of Ti and Cu using Al Kα ($h\nu$ = 1486.6 eV, 150 W, 500 μm of beam spot) as the incident radiation source, and the detected binding energy was calibrated by carbon (C 1s = 284.8 eV).

Photovoltaic Measurements. The photoelectrical conversion property of Cu-TiO_2 was characterized by short-circuit photocurrent response and external quantum efficiency (EQE) under the irradiation of a full spectrum solar simulator. The short-circuit photocurrent response was recorded in a three-electrode cell on a CHI660D electrochemical workstation (Chenhua, Shanghai) under 100 mW/cm^2 xenon lamp (Newport 96000) with an air mass 1.5 global filter (AM 1.5G, Newport 81904) without external bias electrical potential. A saturated calomel electrode (SCE) was used as reference, a platinum wire as counter, and the Cu-TiO_2/FTO film with an exposed area of 0.50 cm^2 as the working electrode. The aqueous Na_2SO_4 solution (0.1 M) in a Pyres-glass-made vessel was used as the electrolyte throughout the photocurrent and EQE measurements. During the test, the TiO_2

dx.doi.org/10.1021/sc400101p | ACS Sustainable Chem. Eng. 2013, 1, 798−804

film was normal to the incident light, which was changed between on and off every 10 s.

The EQE at different incident wavelengths was evaluated by a system consisting of a xenon lamp (300 W, Model 6258, Newport), a cornerstone 260 monochromator (Model 74125, Newport), a UV silicon detector (Model 70356, Newport), a chopper (Model 75151, Newport), a dual channel RS232 Merlin radiometry system (Model 70100 thru 70105, Newport), and an Oriel amplifier for QE light bias.

RESULTS AND DISCUSSION

Morphologies and Crystal Structures of TiO_2 Nanorods Coated with Cu QDs. As shown in Figure 2, the TiO_2 nanorods were formed perpendicularly to FTO substrates and tetragonal in shape with a square top surface, and the average diameter and length of the TiO_2 nanorods were about 93 nm and 1.05 μm, respectively. The top facets of the undecorated TiO_2 nanorods (Figure 2A) appear to contain many step edges, while the side facets are smooth. Once the Cu QD modification was conducted on the TiO_2 surfaces, the top facets of the nanorods became flattened, the nanorods became adherent to each other, and the side facets demonstrated a rough appearance with vast quantities of minute particles inlaid. This latter observation indicates that the Cu QDs were indeed deposited onto the surfaces of the TiO_2 nanorods by repeated solution dipping and redox treatment. For the EDS analysis (Figure 2E), characteristic X-ray signals for Cu can be detected, and the mass fractions of Ti and Cu are 50.5 and 2.4 wt %; the weight percent of Cu on the surface of TiO_2 nanorods is approximately 2.8 wt %.

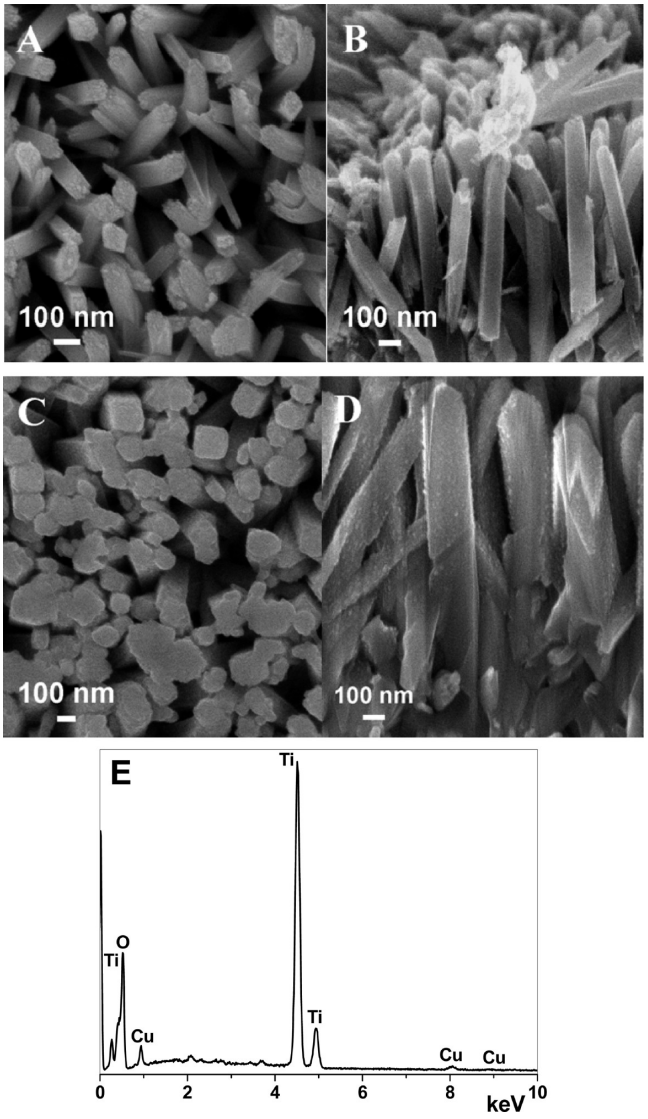

Figure 2. FESEM images of TiO_2 and Cu-TiO_2 nanorod arrays grown on FTO substrates: (A) top view and (B) cross-sectional view of pristine TiO_2 nanorods; (C) top view and (D) cross-sectional view of Cu-TiO_2 nanorods; and (E) EDS spectrum of TiO_2 nanorods coated with Cu QDs (0.05 M Cu^{2+}).

XRD patterns in Figure 3 show the crystal structure of Cu QD-sensitized TiO_2 nanorod arrays. After the products were formed on the FTO substrates, all FTO diffraction peaks were weakened, which can be indexed as tetragonal rutile phase (PDF no. 21-1276). In addition, no obvious XRD differences were observed among the samples with/without the Cu QD sensitization on the TiO_2 surfaces, even with a high Cu^{2+} concentration (0.05 M). Therefore, we can conclude that the formation of Cu QDs has an unremarkable influence on the crystalline structure of the TiO_2 nanorods, and the QDs are thoroughly dispersed on the TiO_2 surfaces.

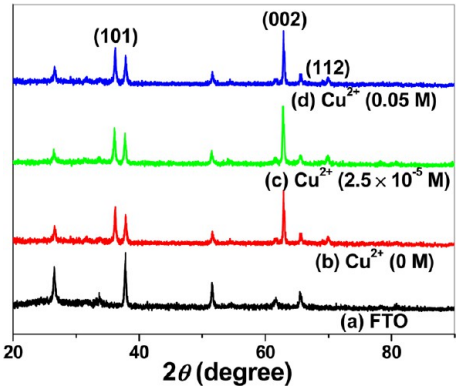

Figure 3. XRD patterns of (a) FTO substrate, (b) pristine TiO_2, (c) Cu-TiO_2 with 2.5×10^{-6} M Cu^{2+} in reactants, and (d) Cu-TiO_2 with 0.05 M Cu^{2+} in reactants.

HRTEM and SAED characterizations were employed to examine the crystal structure and growth direction of the TiO_2 nanorods as well as the particle size of the QDs. As shown in Figure 4A, interplanar spacing of 3.2 ± 0.1 Å (d_{110}) and 2.9 ± 0.1 Å (d_{001}) indicate the formation of the rutile TiO_2 phase (PDF no. 21-1276). The [110] axis is perpendicular to the nanorod side walls, from which one can deduce that the nanorods grow along the [001] direction. In addition, the SAED pattern of symmetrical spots, obtained along the zone axis of $[1\bar{1}1]$, demonstrates that the nanorods exhibit a single-crystal structure (Figure 4B).

Because the surface growth of QDs were limited by the adsorption ability of TiO_2 nanorods to $Cu(NH_3)_4^{2+}$, only a small amount of QDs could be finally obtained and found from the HRTEM image (Figure 4C). Cu QDs with an approximate particle size of 6 nm existed on the surface of TiO_2 nanorods, and the interplanar spacing was 2.1 ± 0.1 Å, which could be indexed to elementary Cu (111) (d = 2.1 Å), CuO (111) (d = 2.3 Å), or Cu_2O (002) (d = 2.1 Å).

In order to clarify the chemical states of Cu QDs, XPS characterizations were conducted. As shown in Figure 5A, the general survey spectrum for Cu QD-modified TiO_2 nanorods

dx.doi.org/10.1021/sc400101p | ACS Sustainable Chem. Eng. 2013, 1, 798−804

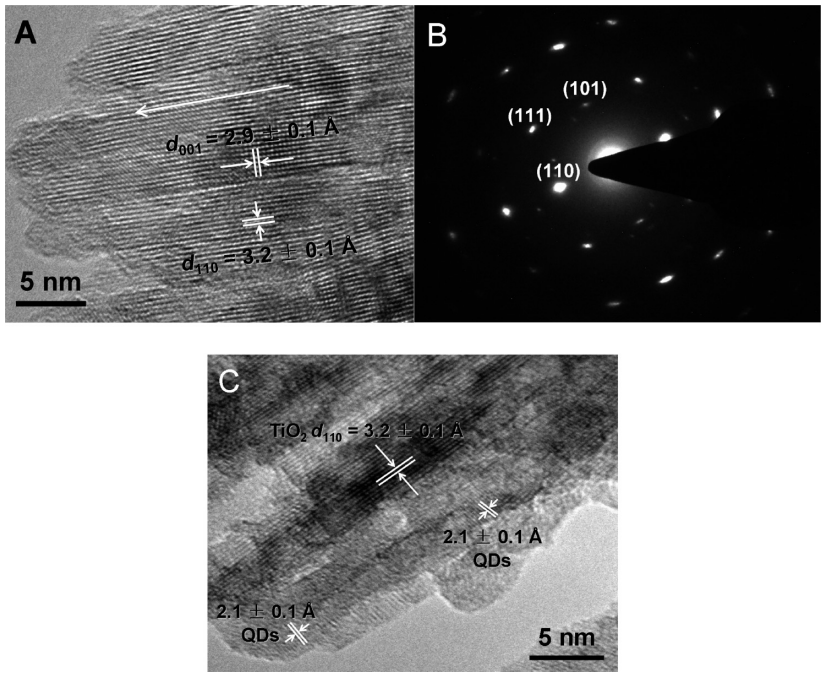

Figure 4. (A) HRTEM image of a single TiO_2 nanorod, in which interplanar crystal spacings are d_{001} = 2.9 ± 0.1 Å and d_{110} = 3.2 ± 0.1 Å. (B) SAED pattern of the same TiO_2 nanorod in part A. (C) HRTEM image of Cu QDs dispersed on TiO_2 nanorod surface.

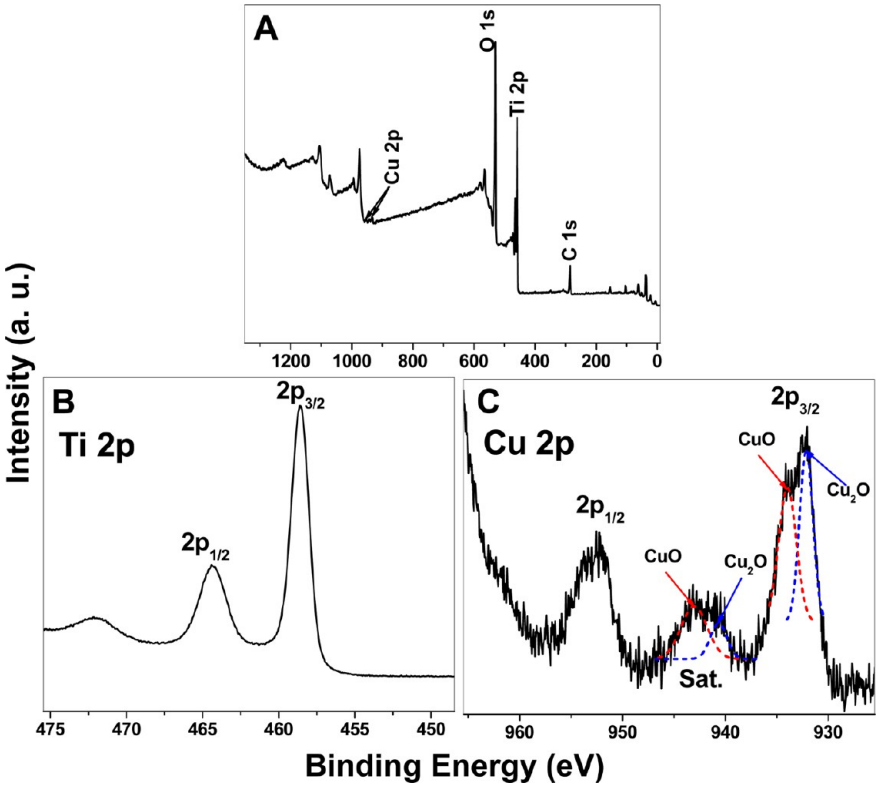

Figure 5. XPS spectrum of Cu QD-sensitized TiO_2 nanorod arrays: (A) survey spectrum, (B) Ti 2p spectrum, and (C) Cu 2p spectrum.

contains Cu, Ti, O, and C elements. The small amount of carbon could have resulted from adventitious hydrocarbons from the XPS instrument itself and can be taken as the standard signal for the correction of other peaks. The binding energy of the superfluous carbon in our detection was C 1s = 285.3 eV, and the standard value should be 284.8 eV. From the Ti 2p spectrum (Figure 5B), two main peaks of Ti $2p_{3/2}$ and $2p_{1/2}$ at bonding energies of 458.0 and 462.8 eV, respectively, reveal that only the Ti^{4+} oxidation state exists on the surface.[36,37] Figure 5C shows a representative signal of spin−orbit split Cu $2p_{3/2}$ and Cu $2p_{1/2}$ with their corresponding shakeup satellites, which indicates that the oxidized copper species were detected on the titania film. Two fitting peaks from Cu $2p_{3/2}$ at around 933.3 and 931.5 eV are observed, which can be assigned to the

dx.doi.org/10.1021/sc400101p | ACS Sustainable Chem. Eng. 2013, 1, 798−804

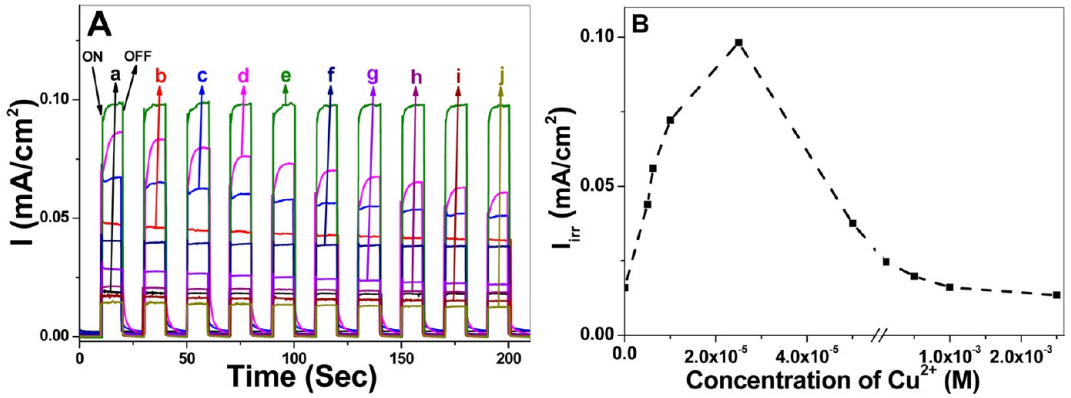

Figure 6. (A) Photocurrent density vs time curves of Cu-TiO_2 nanorod arrays with different Cu^{2+} concentrations in reactants, which were 0, 5.0×10^{-6}, 6.25×10^{-6}, 1.0×10^{-5}, 2.5×10^{-5}, 1.0×10^{-4}, 5.0×10^{-4}, 1.0×10^{-3}, and 2.5×10^{-3} M for curves a–j, respectively. (B) Plot of the instantaneous photocurrent density measured at 95.0 s for each sample in Figure 5A with the original concentration of Cu^{2+}.

Cu(II)[38] state and the Cu(I)[39] state, respectively. In addition, the shakeup satellite peaks around 942.4 and 940.0 eV suggest the existence of fully oxidized Cu(II)O and incompletely oxidized $Cu(I)_2O$.[40] The XPS results above demonstrate that the deposited QDs were actually in the form of CuO or Cu_2O nanoparticles. Once the adsorbed $Cu(NH_3)_4^{2+}$ ions were reduced into elementary Cu by H_2O_2 on the surface of TiO_2, the Cu grains were strongly reductive because of their small size and likely to lose electrons to generate their oxidized form, and the oxidant can be the surrounding adsorbed oxygen.[41] As a result, a mixture of cuprous oxide ($Cu(I)_2O$) and cupric oxide (Cu(II)O) was detected, and the ratio of these two oxides can be influenced by the absorption capability of TiO_2 to O_2. Furthermore, comparing with the bulk oxidized copper compounds, both $2p_{3/2}$ levels of the Cu(II) and Cu(I) shifted toward lower binding energy, which were 933.6 and 932.6 eV for bulk Cu(II)O and $Cu(I)_2O$,[38] respectively, indicating that the species existed as nanocrystalline or quantum dots.[42] The atomic percentage of Ti and Cu are 22.85% and 0.66% in XPS measurements; thus, the weight percentage of Cu on the surface of TiO_2 is approximately 2.3 wt %, consistent with the value obtained from the EDS analysis (2.8 wt %).

Photoelectrical Properties of Cu-TiO_2 Nanorod Arrays. Under irradiation within the appropriate wavelength (E > 3.0 eV), a photoinduced charge separation occurs in TiO_2, and a photocurrent response can be detected in a circuit using an electrochemical workstation. The intensity of the photocurrent represents the charge collection efficiency of the electrode surface and, thereby, can be employed to elucidate the effects of Cu QD sensitization on the photovoltaic performance of TiO_2 nanorod arrays. As given in Figure 6A, for the samples coated with different amounts of Cu QDs, the photocurrents increase to a steady state immediately when the light is on and regresses to zero promptly when the light is off, indicating their excellent sensitivity to the illumination and photoelectrical conversion ability. In addition, the photocurrent response varies widely with the concentration of Cu^{2+}, thus demonstrating that the introduction of Cu QDs has a significant influence on the separation and transportation of the photogenerated charges on the TiO_2 surfaces. In order to clarify the relationship between the photovoltaic performance and the initial concentration of Cu^{2+} more directly, the instantaneous photocurrent densities (I_{irr}) detected at 95.0 s of the samples are listed in Figure 6B. As the concentration of Cu^{2+} in reactants increased, the photocurrent increased initially and then declined. The maximum value reached 98 $\mu A/cm^2$ with 2.5×10^{-5} M of Cu^{2+} in reactants, a value that is >5 times higher than that of the pristine TiO_2 nanorod arrays (16 $\mu A/cm^2$). When excessive QDs were deposited onto the TiO_2 surfaces, the recombination of the photoinduced charges may be aggravated by the aggregation of QDs, and the growth of Cu QDs makes the bandgap smaller and unmatched with TiO_2, both of which can lower the photovoltaic conversion.

Besides the photocurrent response under the solar simulator, external quantum efficiencies (EQE, the spectrally resolved ratio of collected charge carriers to incident photons) of the TiO_2 nanorod arrays decorated with Cu QDs were obtained at different incident wavelengths. In Figure 7, the peak value of

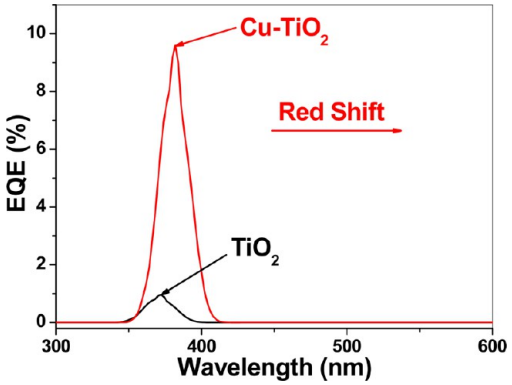

Figure 7. External quantum efficiencies of pristine and Cu QD-modified TiO_2 nanorod films. The concentration of Cu^{2+} was 2.5×10^{-5} M in reactants.

the sensitized TiO_2 (9.6%) is much higher than that of the pristine TiO_2 (0.96%), further suggesting that the participation of Cu QDs improves the photoelectrical conversion ability of TiO_2. In addition, a red shift of the peak is found from 372 to 382 nm after the surface deposition of Cu QDs on TiO_2, possibly resulting from the formation of some narrow bandgap semiconductors (e. g., CuO and Cu_2O). These QD particles seemed to be small enough to have a quantum size effect, by which the increased bandgap energy of QDs matches with that of TiO_2 and subsequently improves the photovoltaic performance of the photoanodes. Moreover, the Pyrex-glass-made vessel cut off the incident light at about 330 nm, which resulted

dx.doi.org/10.1021/sc400101p | ACS Sustainable Chem. Eng. 2013, 1, 798–804

Scheme 1. Configuration of Copper QD-Sensitized TiO_2 Nanorod Arrays on FTO Substrate, the Photoinduced Charge Separation and Transfer between the QDs and TiO_2, and the Energy Level of the Coupled TiO_2/QDs

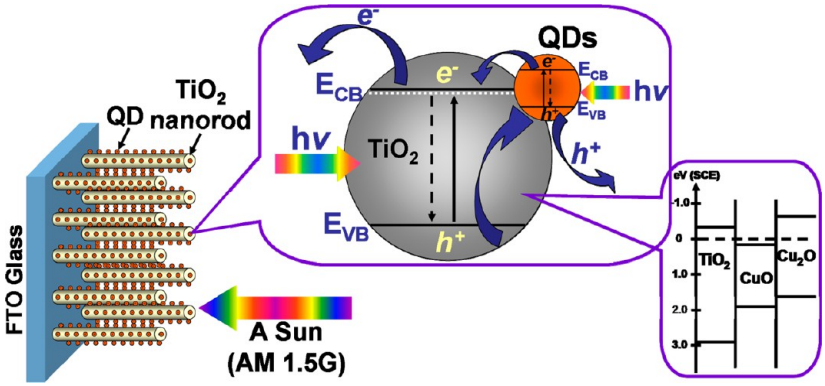

in the photoresponse with a stopping wavelength at around 340 nm.

Plausible Mechanism. When copper QDs were introduced onto the surfaces of TiO_2 nanorods, the surrounding oxygen oxidized the QDs into their high-valence states (e.g., Cu(II) and Cu(I)) afterward. Considering the bandgap energies of bulky Cu(II)O (1.7 eV)[43] and $Cu(I)_2O$ (2.4 eV)[25] as well as the small particle size of QDs, a quantum size effect might produce a wider bandgap for the QDs that consequently matches that of TiO_2. The structure of the photoanode and the photoinduced charge transfer process is illustrated in Scheme 1. When excited by incident photons, the photoelectrons in QDs migrate to the conduction band of TiO_2, and the holes gather in the valence band of the QDs. During this process, the lifetime of the charge carriers can be increased. In addition, one-dimensional single-crystal nanorods favor the directional movement of the photoinduced charges; thus, the recombination of electron−hole pairs is further inhibited, finally resulting in an improved photoelectrical performance.

CONCLUSIONS

In this research, we have synthesized oriented, single-crystal rutile TiO_2 nanorod arrays directly on FTO substrates and then decorated the surface of TiO_2 with Cu quantum dots. We discovered that the oxidation reaction of elementary Cu by the surrounding oxygen occurred after the deposition of the QDs, subsequently producing Cu(II)O and $Cu(I)_2O$ that were dispersed as the copper QDs on the TiO_2 surfaces. For the XRD crystal characterization, little difference could be found between the pristine TiO_2 and the sensitized samples. The Cu QDs could be observed in FESEM images as an abundance of minute grains homogeneously dispersed on the lateral facets of the TiO_2 nanorods, and the particle size measured from the HRTEM image was around 6 nm. Under the irradiation from a solar simulator, the photoelectrical response of the TiO_2 nanorod arrays was enhanced dramatically with the employment of copper QDs. Compared with pristine TiO_2, the optimal short-circuit photocurrent and EQE values of the modified TiO_2 nanorod arrays were increased by more than five and nine times, respectively, indicating the tremendous application potential of copper QDs, having low toxicity and high efficiency, for QDSCs.

AUTHOR INFORMATION

Corresponding Author

*Tel.: +86-532-84022869. Fax: +86-532-84022869. E-mail: DongLifeng@qust.edu.cn.

Notes

The authors declare no competing financial interest.

ACKNOWLEDGMENTS

This work was partially supported by the National Natural Science Foundation of China (51172113), the Research Fund for the Doctoral Program of Higher Education of China (20123719110001), the China Postdoctoral Science Foundation (2012M521297), the Shandong Natural Science Foundation for Distinguished Young Scholars (JQ201118), the Taishan Scholar Overseas Distinguished Professorship program from the Shandong Province Government, PR China, the Shandong Postdoctoral Innovative Program (201203028), the Qingdao Municipal Science and Technology Commission (12-1-4-136-hz), and the Faculty Research Grant and the Sabbatical Leave Award from Missouri State University. The authors also thank Dr. Michael Craig for helpful discussion.

REFERENCES

(1) Yodyingyong, S.; Zhou, X.; Zhang, Q.; Triampo, D.; Xi, J.; Park, K.; Limketkai, B.; Cao, G. Enhanced photovoltaic performance of nanostructured hybrid solar cell using highly oriented TiO_2 nanotubes. *J. Phys. Chem. C* **2010**, *114*, 21851−21855.

(2) Lee, S.; Kim, J. Y.; Youn, S. H.; Park, M.; Hong, K. S.; Jung, H. S.; Lee, J.-K.; Shin, H. Preparation of a nanoporous $CaCO_3$-Coated TiO_2 electrode and its application to a dye-sensitized solar cell. *Langmuir* **2007**, *23*, 11907−11910.

(3) Shao, F.; Sun, J.; Gao, L.; Yang, S.; Luo, J. Template-free synthesis of hierarchical TiO_2 structures and their application in dye-sensitized solar cells. *ACS Appl. Mater. Interfaces* **2011**, *3*, 2148−2153.

(4) Kim, J.-Y.; Sekino, T.; Tanaka, S.-I. Influence of the size-controlled TiO_2 nanotubes fabricated by low-temperature chemical synthesis on the dye-sensitized solar cell properties. *J. Mater. Sci.* **2011**, *46*, 1749−1757.

(5) Sun, W.-T.; Yu, Y.; Pan, H.-Y.; Gao, X.-F.; Chen, Q.; Peng, L.-M. CdS quantum dots sensitized TiO_2 nanotube-array photoelectrodes. *J. Am. Chem. Soc.* **2008**, *130*, 1124−1125.

(6) Wang, H.; Bai, Y.; Zhang, H.; Zhang, Z.; Li, J.; Guo, L. CdS quantum dots-sensitized TiO_2 nanorod array on transparent conductive glass photoelectrodes. *J. Phys. Chem. C* **2010**, *114*, 16451−16455.

(7) Jin, H.; Choi, S.; Velu, R.; Kim, S.; Lee, H. J. Preparation of multilayered CdSe quantum dot sensitizers by electrostatic layer-by-layer assembly and a series of posttreatments toward efficient quantum

dot-sensitized mesoporous TiO_2 solar cells. *Langmuir* **2012**, *28*, 5417−5426.
(8) Nazeeruddin, Kay, A.; Rodicio, I.; Humphry-Baker, R.; Müller, E.; Liska, P.; Vlachopoulos, N.; Grätzel, M. Conversion of light to electricity by *cis*-X_2Bis(2,2′-bipyridyl-4,4′-dicarboxylate)ruthenium(II) charge-transfer sensitizers (X=Cl^-, Br^-, I^-, CN^-, and SCN^-) on nanocrystallineTiO_2 electrodes. *J. Am. Chem. Soc.* **1993**, *115*, 6382−6390.
(9) Nazeeruddin, M. K.; Humphry-Baker, R.; Liska, P.; Grätzel, M. Investigation of sensitizer adsorption and the influence of protons on current and voltage of a dye-sensitized nanocrystalline TiO_2 solar cell. *J. Phys. Chem. C* **2003**, *107*, 8981−8987.
(10) Yella, A.; Lee, H.-W.; Tsao, H. N.; Yi, C.; Chandiran, A. K.; Nazeeruddin, M. K.; Diau, E. W.-G.; Yeh, C.-Y.; Zakeeruddin, S. M.; Grätzel, M. Porphyrin-sensitized solar cells with cobalt (II/III)-based redox electrolyte exceed 12% efficiency. *Science* **2011**, *334*, 629−634.
(11) Lee, W.; Lee, J.; Lee, S.; Yi, W.; Han, S.-H.; Cho, B. W. Enhanced charge collection and reduced recombination of CdS TiO_2 quantum dots sensitized solar cells in the presence of single walled carbon nanotubes. *Appl. Phys. Lett.* **2008**, *92*, 153510.
(12) Peter, L. M.; Riley, D. J.; Tull, E. J.; Wijayantha, K. G. U. Photosensitization of nanocrystalline TiO_2 by self-assembled layers of CdS quantum dots. *Chem. Commun.* **2002**, 1030−1031.
(13) Sambur, J. B.; Riha, S. C.; Choi, D.; Parkinson, B. A. Influence of surface chemistry on the binding and electronic coupling of CdSe quantum dots to single crystal TiO_2 surfaces. *Langmuir* **2010**, *26*, 4839−4347.
(14) Jung, M.-H.; Kang, M. G. Enhanced photo-conversion efficiency of CdSe−ZnS core−shell quantum dots with Au nanoparticles on TiO_2 electrodes. *J. Mater. Chem.* **2011**, *21*, 2694−2700.
(15) Semonin, O. E.; Luther, J. M.; Choi, S.; Chen, H.-Y.; Gao, J.; Nozik, A. J.; Beard, M. C. Peak external photocurrent quantum efficiency exceeding 100% via MEG in a quantum dot solar cell. *Science* **2011**, *334*, 1530−1533.
(16) Dong, C.; Li, X.; Qi, J. First-principles investigation on electronic properties of quantum dot-sensitized solar cells based on anatase TiO_2 nanotubes. *J. Phys. Chem. C* **2011**, *115*, 20307−20315.
(17) Luo, J.; Karuturi, S. K.; Liu, L.; Su, L. T.; Tok, A. L. Y.; Fan, H. J. Homogeneous photosensitization of complex TiO_2 nanostructures for efficient solar energy conversion. *Sci. Rep.* **2012**, *2*, 451.
(18) Etgar, L.; Moehl, T.; Stefanie, G.; Gickey, S. G.; Eychmüller, A.; Grätzel, M. Light energy conversion by mesoscopic PbS quantum dots-TiO_2 heterojunction solar cells. *ACS Nano* **2012**, *6*, 3092−3099.
(19) Tisdale, W. A.; Williams, K. J.; Timp, B. A.; Norris, D. J.; Aydil, E. S.; Zhu, X.-Y. Hot-electron transfer from semiconductor nanocrystals. *Science* **2010**, *328*, 1543−1547.
(20) Yu, P.; Zhu, K.; Norman, A. G.; Ferrere, S.; Frank, A. J.; Nozik, A. J. Nanocrystalline TiO_2 solar cells sensitized with InAs quantum dots. *J. Phys. Chem. B* **2006**, *110*, 25451−25454.
(21) Zaban, A.; Mićić, O. I.; Gregg, B. A.; Nozik, A. J. Photosensitization of nanoporous TiO_2 electrodes with InP quantum dots. *Langmuir* **1998**, *14*, 3153−3156.
(22) Tang, J.; Kemp, K. W.; Hoogland, S.; Jeong, K. S.; Liu, H.; Levina, L.; Furukawa, M.; Wang, X.; Debnath, R.; Cha, D.; Chou, K. W.; Fischer, A.; Amassian, A.; Asbury, J. B.; Sargent, E. H. Colloidal-quantum-dot photovoltaics using atomic-ligand passivation. *Nat. Mater.* **2011**, *10*, 765−771.
(23) Xu, B.; Dong, L.; Chen, Y. Influence of CuO loading on dispersion and reduction behavior of CuO-TiO_2 (anatase) system. *J. Chem. Soc., Faraday Trans.* **1998**, *94*, 1905−1909.
(24) Mor, G. K.; Varghese, O. K.; Wilke, R. H. T.; Sharma, S.; Shankar, K.; Latempa, T. J.; Choi, K.-S.; Grimes, C. A. p-Type Cu-Ti-O nanotube arrays and their use in self-biased heterojunction photoelectrochemical diodes for hydrogen generation. *Nano Lett.* **2008**, *8*, 1906−1911.
(25) Senevirathna, M .K. I.; Pitigala, P. K. D. D. P.; Tennakone, J. Water photoreduction with Cu_2O quantum dots on TiO_2 nanoparticles. *J. Photochem. Photobiol. A: Chem.* **2005**, *171*, 257−259.
(26) Ratanatawanate, C.; Bui, A.; Vu, K.; Balkus, K. J. Low-temperature synthesis of copper(II) sulfide quantum dot decorated TiO_2 nanotubes and their photocatalytic properties. *J. Phys. Chem. C* **2011**, *115*, 6175−6180.
(27) Li, T.-L.; Lee, Y.-L.; Teng, H. $CuInS_2$ quantum dots coated with CdS as high-performance sensitizers for TiO_2 electrodes in photoelectrochemical cells. *J. Mater. Chem.* **2011**, *21*, 5089−5098.
(28) Sun, Q.; Sun, X.; Dong, H.; Zhang, Q.; Dong, L. F. Copper quantum dots on TiO_2: A high-performance, low-cost, and nontoxic photovoltaic material. *J. Renewable Sustainable Energy* **2013**, *5*, 021413.
(29) Liu, B.; Aydil, E. S. Growth of oriented single-crystalline rutile TiO_2 nanorods on transparent conducting substrates for dye-sensitized solar cells. *J. Am. Chem. Soc.* **2009**, *131*, 3985−3990.
(30) Wang, H.; Bai, Y.; Zhang, H.; Zhang, Z.; Li, J.; Guo, L. CdS quantum dots-sensitized TiO_2 nanorod array on transparent conductive glass. *J. Phys. Chem. C* **2010**, *114*, 16451−16455.
(31) Han, Y.; Fan, C.; Wu, G.; Chen, H.-Z.; Wang, M. Low-temperature solution processed utraviolet photodetector based on an ordered TiO_2 nanorod array_polymer hybrid. *J. Phys. Chem. C* **2011**, *115*, 13438−13445.
(32) Sun, X.; Sun, Q.; Zhang, Q.; Zhu, Q.; Dong, H.; Dong, L. F. Significant effects of reaction temperature on morphology, crystallinity, and photoelectrical properties of rutile TiO_2. *J. Phys. D: Appl.* **2013**, *46*, 095102.
(33) Sun, Q.; Sun, X.; Li, Y.; Dong, L. F. Growth and photoelectrical property of TiO_2 nanorods with an array-cluster double-layer structure. *Chin. J. Lumin.* **2013**, *34*, 61−65.
(34) Sun, Q.; Sun, X.; Li, Y.; Yu, L.; Dong, L. F. Correlations between morphology and photoelelctrcal properties of single-crystal rutile TiO_2 nanorods. *Sci. Adv. Mater.* **2013**, *5*, 1−9.
(35) Li, G.; Dimitrijevic, N. M.; Chen, L.; Rajh, T.; Gray, K. A. Role of surface/interfacial Cu^{2+} sites in the photocatalytic activity of coupled CuO-TiO_2 nanocomposites. *J. Phys. Chem. C* **2008**, *112*, 19040−19044.
(36) Tian, H.; Hu, L.; Zhang, C.; Liu, W.; Huang, Y.; Mo, L.; Guo, L.; Sheng, J.; Dai, S. Retarded charge recombination in dye-Sensitized nitrogen-doped TiO_2 solar cells. *J. Phys. Chem. C* **2010**, *114*, 1627−1632.
(37) Cao, J.-L.; Shao, G.-S.; Ma, T.-Y.; Wang, Y.; Ren, T.-Z.; Wu, S.-H.; Yuan, Z.-Y. Hierarchical meso−macroporous titania-supported CuO nanocatalysts: preparation, characterization and catalytic CO oxidation. *J. Mater. Sci.* **2009**, *44*, 6717−6726.
(38) Espinós, J. P.; Morales, J.; Barranco, A.; Caballero, A.; Holgado, J. P.; González-Elipe, A. R. Interface effects for Cu, CuO, and Cu_2O deposited on SiO_2 and ZrO_2. XPS determination of the valence state of copper in Cu/SiO_2 and Cu/ZrO_2 catalysts. *J. Phys. Chem. B* **2002**, *106*, 6921−6929.
(39) Borgohain, K.; Murase, N.; Mahamuni, S. Synthesis and properties of Cu_2O quantum particles. *J. Appl. Phys.* **2002**, *92*, 1292−1297.
(40) Chusuei, C. C.; Brookshier, M. A.; Goodman, D. W. Correlation of relative X-ray photoelectron spectroscopy shake-up intensity with CuO particle size. *Langmuir* **1999**, *15*, 2806−2808.
(41) Dong, L. F.; Yu, L. Y.; Cui, Z. L.; Dong, H. Z.; Ercius, P.; Song, C. Y.; Duden, T. Direct imaging of copper catalyst migration inside helical carbon nanofibers. *Nanotechnology* **2012**, *23*, 035702.
(42) Nanda, J.; Kuruvilla, B. A.; Sarma, D. D. Photoelectron spectroscopic study of CdS nanocrystallites. *Phys. Rev. B* **1999**, *59*, 7473−7479.
(43) Bandara, J.; Udawatta, C. P. K.; Rahapakse, C. S. K. Highly stable CuO incorporated TiO_2 catalyst for photocatalytic hydrogen production from H_2O. *Photochem. Photobiol. Sci.* **2005**, *4*, 857−861.